ISSN 0030-400X, Optics and Spectroscopy, 2008, Vol. 104, No. 5, pp. 767–771. © Pleiades Publishing, Ltd., 2008.
Original Russian Text © D.V. Ushakov, I.S. Manak, 2008, published in Optika i Spektroskopiya, 2008, Vol. 104, No. 5, pp. 846–851.

LASERS AND THEIR APPLICATIONS

Energy and Emission Characteristics of Superlattice Quantum-Cascade Structures

D. V. Ushakov and I. S. Manak

Belarussian State University, pr. Nezavisimosti 4, Minsk, 220030 Belarus

e-mail: UshakovDV@bsu.by

Received February 22, 2007; in final form, November 19, 2007

Abstract—Energy levels, wave functions, and matrix elements of optical dipole transitions have been numerically calculated for superlattice quantum-cascade structures. An expression for the gain has been obtained with regard to the complete set of energy levels in different models of spectral-line broadening. A universal relation between the gain and emission spectra for unipolar laser structures has been proposed. The effect of spectral broadening on the shape of emission spectra is estimated. The electroluminescence spectra are compared with the calculated spontaneous recombination spectra and good agreement between the results is shown.

PACS numbers: 78.20.Bh, 78.67.Pt

DOI: 10.1134/S0030400X08050202

INTRODUCTION

Intense investigations aimed at developing mid-IR semiconductor lasers have been carried out in view of great possibilities of their practical application. Mass production of compact reliable light sources (which can be used in high-precision chemical analysis aimed at finding contamination regions in atmosphere and in open optical communication in telecommunication and location) is possible on the basis of IR lasers. Such lasers are ideal for spectroscopic applications. Long-wavelength lasers are widely used in medicine and medical diagnostics.

Studies on development of semiconductor IR lasers are carried out in the following main directions: investigation of physics of intraband transitions in unipolar superlattice quantum-cascade lasers [1–9], attainment of generation at the difference frequency in semiconductor quantum-confined heterostructures emitting simultaneously at two wavelengths [10, 11], analysis of interband generation in narrow-gap heterostructures, and study of the physics of bipolar superlattice quantum-cascade structures [12, 13].

In 1972, Kazarinov and Suris [1] proposed for the first time the concept of unipolar quantum-cascade lasers based on optical transitions between subbands within one energy (conduction) band. It was theoretically predicted that, as a result of cascade arrangement of active layers, after reaching the threshold, each injected electron can form N laser photons upon transmission through N structure cascades. The first quantum-cascade lasers were developed in 1994 by Capasso's team [2]. These lasers operated on radiative transitions between the states in double quantum wells (QWs), and the pumping mechanism was resonant tunneling of electrons. The population inversion between the states involved in induced transitions was obtained by decreasing the lifetime of the final state with the use of resonant emission of optical phonons and increasing the lifetime of the initial states through suppression of tunneling from these levels with the use of an electron Bragg reflector. In 1997, superlattice quantum-cascade lasers with radiative transitions between energy minibands were developed [3]. A significant increase in power and a decrease in the threshold current of quantum-cascade lasers is obtained using an active region with a set of QWs and barrier layers with a gradually changing period (chirped superlattices) [6], as well as by introducing additional doped n–i–p–i layers [8]. Room temperature cw quantum-cascade lasers with level–miniband (bound-to-continuum) transitions have been developed on the basis of superlattices [9].

Modern quantum-cascade lasers are based on complex structures with several tens of repeating cascades (periods), grown by molecular-beam epitaxy. Each cascade is, in turn, a set of potential wells and barriers. Currently, quantum-cascade lasers operate in the range of 3–160 μm. The lasing range is mainly determined by the thicknesses of quantum-confinement layers, doping level, and potential-barrier height ΔE_c in the conduction band. The compounds used for quantum-cascade lasers (that are known to date) and the structures of active regions are shown in Fig. 1.

The emission spectra of quantum-cascade lasers based on AlInAs/GaInAs and Si/SiGe heterostructures lie, respectively, in the ranges 3.6–83 μm [2–8, 14] and 7.5–9.5 μm [15–17]. The emission range of GaAs/AlGaAs-based quantum-cascade lasers ranges from 8 μm to several terahertz (~88 μm) [18–21]. The use of a sequence of narrow- and wide-gap InAs/AlSb-

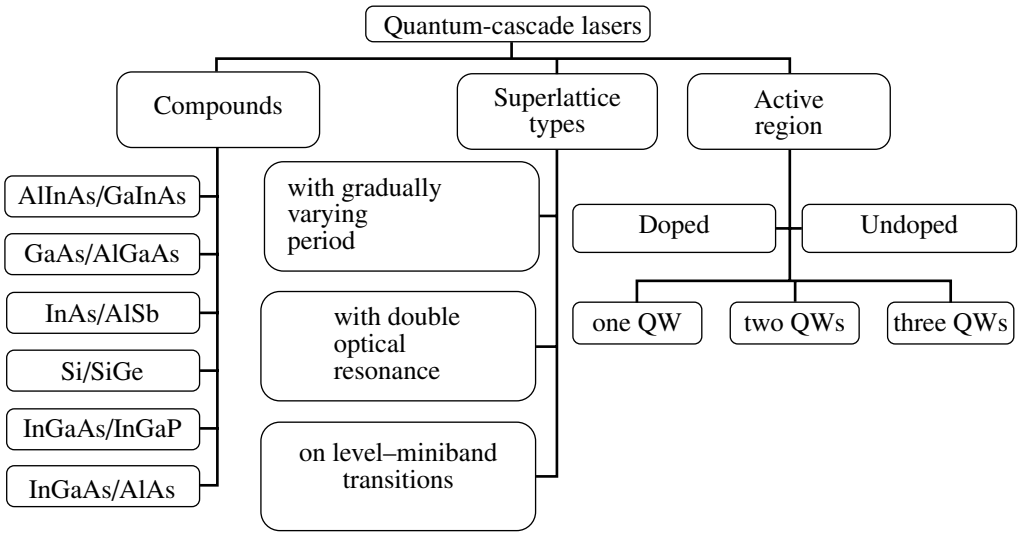

Fig. 1. Classification of quantum-cascade lasers.

based compounds allows one to increase the potential-barrier height to $\Delta E_c \approx 2$ eV in the conduction band; such an increase is promising for developing short-wavelength quantum-cascade lasers in the range 2–5 μm [22]. The structures based on InGaAs/InGaP layers grown on GaAs [23] and InGaAs/AlAs [24] substrates are also alternative compounds for short-wavelength quantum-cascade lasers.

Precise control of such design parameters as the thickness and doping level of layers and the use of new semiconductor compounds make it possible to develop quantum-cascade lasers with new functional possibilities and improved characteristics. However, high technological cost makes necessary preliminary theoretical investigations of the parameters of such lasers. To date, in the theory of amplification and emission of light in heterostructures with quantum-confinement layers, the questions related to the choice of the spectral-line broadening profile remain unsolved [25–27]. Generally, the Lorentzian emission-line shape is used in calculation of gain spectra [28, 29]. A theory for calculating luminescence spectra in quantum-cascade structures is absent. Theoretical estimates are reduced to integration of the strength of an oscillator with a Lorentzian emission-line shape [30]. This study is devoted to more detailed consideration of the above-mentioned questions.

ENERGY-BAND DIAGRAM, ENERGY LEVELS, AND WAVE FUNCTIONS

The potential profile for electrons in quantum-cascade heterostructures composed of materials with different arrangement and width of energy bands is a set of potential wells and barriers in the direction transverse to the layer plane; the electron energies and momenta are quantized in potential wells. As a result, in the case of transverse motion of electrons through the system of wells and barriers, resonant-current effects are observed due to the interference of the electron waves reflecting from the interfaces of neighboring layers [31, 32]. For the electrons with transverse energies coinciding with the energies of some resonant levels, the barrier penetrability greatly increases, and barriers almost do not affect a particle passing through them. The energies and wave functions for a system of potential wells and barriers of an arbitrary shape were determined by solving the stationary Schrödinger equation [33]

$$-\frac{\hbar^2}{2}\frac{d}{dz}\left(\frac{1}{m^*(z, E_c(z))}\frac{d\psi_n(z)}{dz}\right) - (E_n - E_c(z))\psi_n(z) = 0, \quad (1)$$

where E_n are quantum-confinement levels, $\psi_n(z)$ are the wave function envelopes, and $E_c(z)$ is the potential energy profile for the conductivity band in an electric field.

Figure 2 show the results of numerical calculations of the energy-band diagram of the conduction band $E_c(z)$ and the squared moduli of the electron wave functions for two periods of an $Al_{0.48}In_{0.52}As$–$Ga_{0.47}In_{0.53}As$ superlattice structure in the electric field $E = 3.5 \times 10^6$ V m^{-1}. The calculations were performed on the basis of the transfer-matrix method [33, 34] within the extended Bastard model, taking into account the coordinate and energy dependences of the electron effective mass $m^*(z, E_c(z))$ [33]. In this case, the potential-barrier height in the conduction band was assumed to be $\Delta E_c = 0.51$ eV, and the calculated (according to [33]) effective masses of charge carriers were $m^* = 0.073m_0$ for

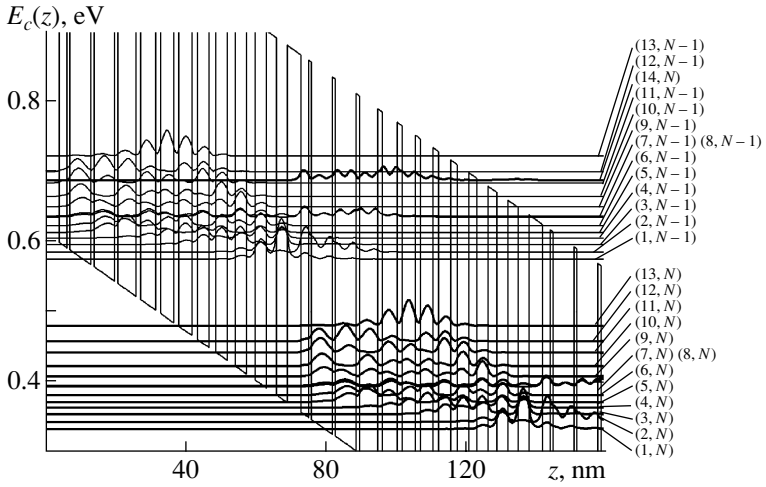

Fig. 2. Energy diagram of the conduction band $E_c(z)$ and the squared moduli of the electron wave functions calculated for two cascades of the $Al_{0.48}In_{0.52}As$–$Ga_{0.47}In_{0.53}As$ superlattice structure in the electric field $E = 3.5 \times 10^6$ V m^{-1}. The layer thicknesses from left to right are 3.9, **2.2**, 0.8, **6.0**, 0.9, **5.9**, 1.0, **5.2**, 1.3, **4.3**, 1.4, **3.8**, 1.5, **3.6**, 1.6, **3.4**, 1.9, **3.3**, 2.3, **3.2**, 2.5, **3.2**, 2.9, and **3.1** nm. In the entire sequence of layers, $Ga_{0.47}In_{0.53}As$ QWs are indicated in bold. The enumeration of the energy levels is shown on the right.

$Al_{0.48}In_{0.52}As$ barrier layers and $m^* = 0.041m_0$ for $Ga_{0.47}In_{0.53}As$ QWs. It can be seen in Fig. 2 that, upon transition from one period to another, the wave functions are repeated and may lie within several periods of the quantum-cascade structure. Two successive periods of the structure (for example, $N-1$ and N) are generally sufficient to calculate the spectral characteristics of quantum-cascade lasers. We will arbitrarily enumerate the energy levels so that to cover all nonrepeating wave functions belonging to one period. Such enumeration is convenient for further calculations of level populations in subbands, as well as gain and emission spectra of quantum-cascade structures.

CALCULATION OF EMISSION CHARACTERISTICS

One can obtain an expression for the gain of unipolar quantum-cascade structures, taking into account the chosen shape of emission line broadening, by integrating the product of the δ function and the broadening profile. In this case, the expression for the gain g in the case of intrasubband transitions as a function of the light frequency ν in the multilevel approximation can be written as

$$g(\nu) = \sum_n \sum_m g_{nm}(\nu)$$
$$= e^2/(\hbar^3 \varepsilon_0 c n_r d) \sum_n \sum_m m_{fm} |z_{nm}|^2 \int_{E_{fm}}^{\infty} dE_f (E_i - E_f) \quad (2)$$
$$\times F[h\nu - (E_i - E_f), \gamma](f(E_i - F_n) - f(E_f - E_m)),$$

where $E_i = (E_f - E_{fm})m_{fm}/m_{in} + E_{in}$, $z_{nm} = \int \psi_n^* z \psi_m dz$ is a matrix element of dipole transitions, F_n and F_m are the quasi-Fermi levels in minibands n and m with the energies E_{in} and E_{fm} and the effective masses m_{in} and m_{fm}, d is the thickness of the quantum-cascade structure, n_r is the refractive index, c is the speed of light, and $f(E) = [\exp(E/kT) + 1]^{-1}$ is the Fermi–Dirac distribution function. In unipolar quantum-cascade lasers, optical transitions occur between energy levels in each period, as well as between levels in different periods. Therefore, all possible transitions for two periods in a quantum-cascade laser are taken into account in (2), and summation is over all quantum numbers of the initial (n) and final (m) states, for which $E_{in} - E_{fm} > 0$. The function $F(\Delta E, \gamma)$ with the broadening parameter γ describes the emission-line profile and is most often used in the form

$$F(\Delta E, \gamma)$$
$$= \begin{cases} \gamma_L/\pi(\Delta E^2 + \gamma_L^2) & \text{Lorentzian,} \\ 1/(\sqrt{\pi}\gamma_G)\exp(-\Delta E^2/\gamma_G^2) & \text{Gaussian,} \\ (\pi\gamma_U \cosh[\Delta E/(2\gamma_U)])^{-1} & \text{exponential [35],} \\ (4\gamma_E \cosh^2[\Delta E/(2\gamma_E)])^{-1} & \text{exponential [27].} \end{cases} \quad (3)$$

According to the experimental observations [25–27], the broadening profile of the spectral line is asymmetric. The asymmetry of the spectral broadening profile is related to the non-Markovity of the relaxation process and dependence of the lifetime on the carrier energy [25–27]. The simplest mixed model of emission line broadening was proposed in [36], where an asym-

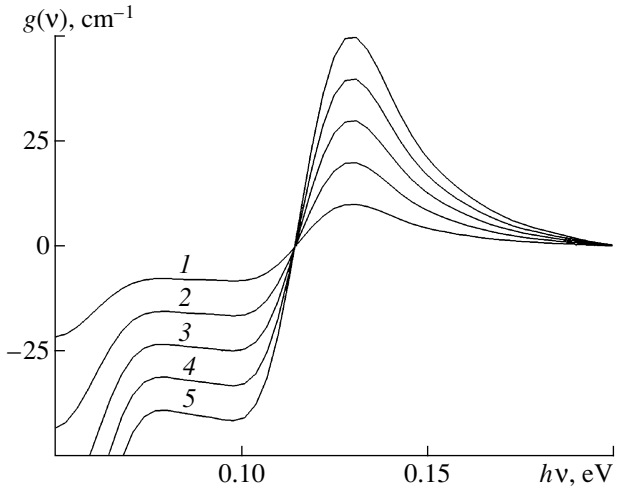

Fig. 3. Gain spectra of the superlattice quantum-cascade structure, calculated within the model of Gaussian line broadening with the broadening parameter γ_G = 15 meV. The numbers at curves correspond to different total surface electron concentrations in a cascade: n_{stot} = (*1*) 10^{11}, (*2*) 2×10^{11}, (*3*) 3×10^{11}, (*4*) 4×10^{11}, and (*5*) 5×10^{11} cm^{-2}.

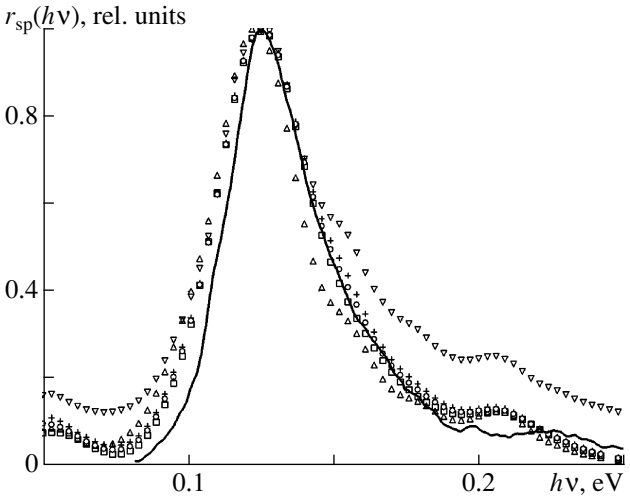

Fig. 4. Electroluminescence spectra reported in [30] (bold line) in comparison with the spontaneous emission spectra of the superlattice quantum-cascade structure, calculated within the Gaussian (□), Lorentzian (▽), mixed (△), and exponential [27] (+) and [35] (○) models of broadening line profiles with the broadening parameter γ_G = 15 meV.

metric broadening profile (whose portions at $\Delta E < 0$ and $\Delta E > 0$ are described by the Lorentzian and Gaussian curves, respectively) was investigated.

It is known that, upon interband (conduction band – valence band) transitions in semiconductors, the spontaneous recombination rate $r_{sp}(h\nu)$ and the gain $g(\nu)$ are related by a universal relation [37]. By analogy with [37] and with allowance for the intrasubband character of optical transitions, we obtain the following universal relation between the gain $g(\nu)$ and spontaneous recombination rate $r_{sp}(h\nu)$ for unipolar quantum-cascade lasers:

$$r_{sp}(h\nu) = v_g \rho(h\nu) \times \sum_n \sum_m \frac{g_{nm}(\nu)}{1 - \exp\{[(E_n - E_m) - (F_n - F_m)]/kT\}}, \quad (4)$$

where $\rho(h\nu) = (h\nu)^2 n_r^2 / (\pi^2 c^2 \hbar^3 v_g)$ is the density of electromagnetic modes and v_g is the speed of light in the crystal. Previously, a similar expression was obtained [34] for a simpler two-level scheme of transitions in quantum-cascade lasers.

RESULTS AND DISCUSSION

Calculations of the emission characteristics of superlattice quantum-cascade structures were performed within different models of emission line broadening. The broadening parameter γ_G was set for the Gaussian emission line, and the other broadening parameters were found from the equality of all broadening functions $F(\Delta E, \gamma)$ in the maximum. Calculation of the populations of the energy levels and the corresponding quasi-Fermi levels was performed on the basis of numerical solution of the system of balance equations [38]. The calculated emission spectra are shown in Figs. 3 and 4.

The results of the calculations indicate that the fundamental transitions for the structure studied lie in the energy range 120–130 meV and correspond to two optical transitions of electrons: the transition from the first level of period $(N-1)$ to the 12th level of period N, i.e., the $(1, N-1)$–$(12, N)$ and $(2, N-1)$–$(12, N)$ transitions (Figs. 2–4). The dominance of these transitions is related to the highly inverted level population and the large matrix elements z_{nm} of the dipole transitions. For example, the surface electron concentrations at the levels $(1, N-1)$, $(2, N-1)$, and $(12, N)$ are 8.0×10^{10}, 3.8×10^{10}, and 4.3×10^9 cm^{-2}, respectively, and the matrix elements of the $(1, N-1)$–$(12, N)$ and $(2, N-1)$–$(12, N)$ dipole transitions are 1.1 and 1.4 nm, respectively. Note that, with an increase in the excitation level of quantum-cascade lasers (which is determined by the emitter doping), the gain maximum increases, whereas the wavelength in the maximum almost does not change and is equal to ~9.5 μm.

To establish the applicability of the theoretical model for describing the emission spectra of quantum-cascade lasers, we will perform comparison with the electroluminescence spectra measured at T = 300 K [30]. As can be seen in Fig. 4, the Gaussian, mixed, and exponential models of emission line broadening describe in the best way the experimental spectra. The Lorentzian model of emission line broadening is least appropriate to describe the emission spectra. The rea-

son is that the spontaneous recombination rate r_{sp} linearly increases with an increase in the photon energy $h\nu$ at high frequencies. Therefore, the total recombination rate cannot be found, since the integral $\int r_{sp}(h\nu)d(h\nu)$ diverges. To make the integral of $r_{sp}(h\nu)$ convergent, according to expressions (2)–(4), the broadening function $F(\Delta E)$ of the emission line at high photon energies should decrease faster than $(h\nu)^{-3}$. As follows from formulas (2)–(4), this condition is satisfied for the Gaussian, mixed, and exponential models of line broadening.

CONCLUSIONS

A complex analysis of the spontaneous emission and gain spectra of superlattice quantum-cascade structures has been performed. Analytical expressions for the gain and spontaneous recombination rate have been obtained with regard to the emission line broadening. Good agreement between the result of numerical calculations of the emission spectra and the experimental data is demonstrated.

ACKNOWLEDGMENTS

We are grateful to V.K. Kononenko and A.A. Afonenko for the discussion of the results and help. This study was supported by the Belarussian Republican Foundation for Basic Research.

REFERENCES

1. R. A. Kazarinov and R. A. Suris, Fiz. Tekh. Poluprovodn. (Leningrad) **6** (1), 148 (1972) [Sov. Phys. Semicond. **6**, 120 (1972)].
2. J. Faist, F. Capasso, D. L. Sivco, et al., Science **264**, 553 (1994).
3. G. Scamarcio, F. Capasso, J. Faist, et al., Appl. Phys. Lett. **70** (14), 1796 (1997).
4. J. Faist, A. Tredicucci, F. Capasso, et al., IEEE J. Quantum Électron. **34** (2), 336 (1998).
5. G. Scamarcio, C. Gmachl, F. Capasso, et al., Semicond. Sci. Technol. **13** (11), 1333 (1998).
6. A. Tredicucci, F. Capasso, C. Gmachl, et al., Appl. Phys. Lett. **73** (15), 2101 (1998).
7. F. Capasso, A. Tredicucci, C. Gmachl, et al., IEEE J. Sel. Top. Quantum Électron.**5** (3), 792 (1999).
8. J. Faist, A. Müller, M. Beck, et al., IEEE Photonics Technol. Lett. **12** (3), 263 (2000).
9. J. Faist, M. Beck, T. Aellen, and E. Gini, Appl. Phys. Lett. **78** (2), 147 (2001).
10. V. Ya. Aleshkin, A. A. Afonenko, and N. B. Zvonkov, Fiz. Tekh. Poluprovodn. (St. Petersburg) **35** (10), 1256 (2001) [Semiconductors **35**, 1203 (2001)].
11. A. A. Afonenko, V. Ya. Aleshkin, and A. A. Dubinov, Semicond. Sci. Technol. **20** (5), 357 (2005).
12. B. H. Yang, D. Zhang, R.-Q. Yang, et al., Appl. Phys. Lett. **72** (18), 2220 (1998).
13. G. G. Zegrya, Sorosovskiĭ Obrazovatel'nyĭ Zh. **7** (6), 70 (2001).
14. L. Ajili, G. Scalari, N. Hoyler, et al., Appl. Phys. Lett. **87**, 141 107-1 (2005).
15. G. Dehlinger, L. Diehl, U. Gennser, et al., Science **290**, 2277 (2000).
16. I. Bormann, K. Brunner, S. Hackenbuchner, et al., Appl. Phys. Lett. **80** (13), 2260 (2002).
17. L. Diehl, S. Mentes, E. Müller, et al., Appl. Phys. Lett. **81** (25), 4700 (2002).
18. C. Sirtori, P. Kruck, S. Barbieri, et al., Appl. Phys. Lett. **73**, 3486 (1998).
19. C. Sirtori, P. Kruck, S. Barbieri, et al., Appl. Phys. Lett. **75** (25), 3911 (1999).
20. M. Rochat, L. Ajili, H. Willenberg, et al., Appl. Phys. Lett. **81** (8), 1381 (2002).
21. G. Scalaria, N. Hoyler, M. Giovannini, and J. Faist, Appl. Phys. Lett. **86**, 181 101-1 (2005).
22. J. Devenson, D. Barate, O. Cathabard, et al., Appl. Phys. Lett. **89**, 191 115-1 (2006).
23. M. P. Semtsiv, G. G. Tarasov, W. T. Masselink, et al., Appl. Phys. Lett. **82** (20), 3418 (2003).
24. M. Semtsiv, M. Ziegler, S. Dreβler, et al., Appl. Phys. Lett. **85** (9), 1478 (2004).
25. M. Yamanishi and Y. Lee, IEEE J. Quantum Électron. **23** (4), 367 (1987).
26. M. Asada, IEEE J. Quantum Électron. **25** (9), 2019 (1989).
27. P. G. Eliseev and I. V. Akimova, Fiz. Tekh. Poluprovodn. (St. Petersburg) **32** (4), 478 (1998) [Semiconductors **32**, 428 (1998)].
28. V. B. Gorfinkel, S. Luryi, and B. Gelmont, IEEE J. Quantum Electron. **32** (11), 1995 (1996).
29. S.-C. Lee and A. Wacker, Phys. Rev. B: Condens. Matter Mater. Phys. **66** (24), 245 314-1 (2002).
30. R. Maulini, M. Beck, J. Faist, and E. Gini, Appl. Phys. Lett. **84** (10), 1659 (2004).
31. L. V. Iogansen, Zh. Tekh. Fiz. **45**, 207 (1963).
32. L. Chang, L. Esaki, and R. Tsu, Appl. Phys. Lett. **24** (12), 593 (1974).
33. K. H. Yoo, L. R. Ram-Mohan, and D. F. Nelson, Phys. Rev. B: Condens. Matter Mater. Phys. **39** (17), 12 808 (1989).
34. D. V. Ushakov and A. A. Afonenko, *Low-Dimensional Systems-2. Physics and Chemistry of Elements and Systems with Low-Dimensional Structurization* (*Obtainment, Diagnostics, and Application of New Materials and Structures*) (Grodno: Izd-vo Grodn. Gos. Univ., 2003), No. 3, p. 29.
35. R. Singolani, W. Stolz, and K. Ploog, Phys. Rev. B: Condens. Matter Mater. Phys. **40** (5), 2950 (1989).
36. V. K. Kononenko, I. S. Manak, S. V. Nalivko, et al., Zh. Prikl. Spektrosk. **64** (2), 221 (1997).
37. V. P. Gribkovskiĭ, *Theory of Light Absorption and Emission in Semiconductors* (Nauka i Tekhnika, Minsk, 1975) [in Russian].
38. D. V. Ushakov and I. S. Manak, Zh. Prikl. Spektrosk. **74** (6), 801 (2007).

Translated by Yu. Sin'kov